# Adaptive Finite Volume Schemes for Conservation Laws based on Local Multiresolution Techniques

Birgit Gottschlich–Müller and Siegfried Müller

**Abstract.** A new adaptive strategy for finite volume schemes is presented based on local multiscale decompositions. By this approach, the complexity of the scheme can be restricted to the number of significant coefficients. For one–dimensional, scalar conservation laws, the efficiency of the concept is verified for several test configurations.

## 1. Introduction

We consider partial differential equations of the form

$$\frac{\partial\, u(t,x)}{\partial\, t} + \frac{\partial\, f(u(t,x))}{\partial\, x} = 0, \qquad 0 < t < T,\ a < x < b \tag{1}$$

with $T > 0$ and $a, b \in \mathrm{I\!R}$ fixed, the so–called conservation laws. Herein, $u : [a,b] \to \mathrm{I\!R}$ is the conservative quantity and $f : \mathrm{I\!R} \to \mathrm{I\!R}$ the flux. In order to ensure a unique solution, an initial condition $u(0,x) = u_0(x),\ a < x < b$, has to be imposed. In practical applications, boundary conditions of the form $g_a(u(t,a)) = 0,\ g_b(u(t,b)) = 0,\ 0 \le t \le T$ are also needed. The one–dimensional scalar equation (1) is a simple model for more complex systems arising from fluid dynamics, e.g. Euler equations.

During the last decade, finite volume schemes have been proven to be very robust and reliable approximation schemes for conservation laws as has been verified by numerous applications. However, the construction of robust and efficient schemes is not yet finished. More advanced approaches are based on the heterogeneity of the flow field, i.e., several physical effects proceeding on different spatial and temporal scales have to be appropriately resolved. In order to resolve these effects by a numerical scheme, different discretization lengths are required where the highest resolution is determined by the finest scale. In the case of multidimensional flow fields this will, in general, exceed presently available memory capacities or computational time will become prohibitively long. Therefore, algorithms have to be developed with computational effort and memory capacity proportional to the complexity of the underlying problem, i.e., only in regions where small–scale effects are present the discretization has to be chosen sufficiently fine, and elsewhere a much coarser discretization will be sufficient. In view of realistic simulations of multidimensional flow fields around complex geometries uniform discretizations are no longer adequate since they exceed presently accessible resources of modern computer systems. In principle, new computer generations will not overcome this problem. Therefore, discretizations have to be adaptive rather than uniform, in order to utilize efficiently the available resources. Nowadays, numerous software packages especially applied in engineering are not in general based on adaptive strategies, although adaptive concepts are developed and investigated for some time in basic research. Herein, adaptivity is controlled by local gradients since error estimates are, in general, not available for problems of interest in practice. The quantity by which adaptivity is performed depends, in general, on the problem configuration at hand. Considering another problem, this quantity can turn out to be useless. Hence, concepts which are independent of the underlying problem have to be developed, i.e., concepts which can be universally applied and are capable to resolve the different scales. To this end, techniques are required by which information can be decomposed into the different scales. A well–known example is the Fourier expansion of a signal. More advanced techniques are based on wavelets. The incorporation of wavelets into the discretization of partial differential equations is subject of current research, yet it is still in the beginning, at least as far as applications in engineering are concerned.

In the present paper, we introduce an new concept how to incorporate multiscale techniques into already existing finite volume schemes in order to achieve a genuinely adaptive scheme. This approach represents a significant extension of recent investigations in this field based on hybrid techniques (cf. [5, 7, 1, 4]). Firstly, we describe a multiscale decomposition applied to cell averages. This decomposition is incorporated into an arbitrary finite volume scheme. Several test calculations have been performed verifying the efficiency of our adaptive strategy. In the end, we give a short outlook on future work and possible improvements.

## 2. Multiscale Decomposition

In the following, we summarize the derivation of a multiscale decomposition for a sequence of discrete averages corresponding to an integrable function $u : \Omega \to \mathbb{R}$ defined on $\Omega$ representing the computational domain. In our applications, we choose $\Omega = [a, b] \subset \mathbb{R}$. However, the presented concept also holds for $\Omega \subset \mathbb{R}^d,\ d > 1$. The starting point is a sequence of $L + 1$ decompositions of $\Omega$ corresponding to increasingly higher resolution, i.e., $\Omega = \bigcup_{j\in I_k} V_{k,j},\ k = 0, \ldots, L$, where $k$ indicates the level of resolution with $k = 0$ denoting the coarsest discretization and $k = L$ the finest, and $j$ represents the position of the cell corresponding to this level. The only assumption we have to impose on this decomposition is the nestedness of the sequence, i.e., $V_{k,j} = \bigcup_{l\in D_{k,j}} V_{k+1,l},\ D_{k,j} \subset I_{k+1},\ j \in I_k$, which means that a coarse–grid cell is composed of $\#D_{k,j}$ fine–grid cells. To any of these cells we now define the cell average

$$u_{k,j} := \frac{1}{|V_{k,j}|} \int_{V_{k,j}} u(x)\ dV, \quad j \in I_k,\ k = 0, \ldots, L. \tag{2}$$

The main task is to determine a completion of $\mathrm{IR}^{\# I_k}$ to $\mathrm{IR}^{\# I_{k+1}}$ such that

$$u_{k+1,j} = \sum\nolimits_{r \in I_k} m_{j,r}^{k,0}\, u_{k,r} + \sum\nolimits_{r \in J_k} m_{j,r}^{k,1}\, d_{k,r}, \quad j \in I_{k+1}, \tag{3}$$

holds and there exist coefficients $g_{j,r}^{k,0}$ and $g_{j,r}^{k,1}$ such that

$$u_{k,j} = \sum\nolimits_{r \in I_{k+1}} g_{j,r}^{k,0}\, u_{k+1,r}, \quad j \in I_k, \tag{4}$$

$$d_{k,j} = \sum\nolimits_{r \in I_{k+1}} g_{j,r}^{k,1}\, u_{k+1,r}, \quad j \in J_k, \tag{5}$$

where $J_k$ is the index set corresponding to the coefficients $d_{k,j}$ such that $\# J_k = \# I_{k+1} - \# I_k$. The coefficients $d_{k,j}$ may be seen as difference information between the data of level $k$ and $k+1$, which can be interpreted as prediction error.

From a numerical point of view, we have to impose four reasonable conditions to the coefficients of $\mathbf{M}_{k,i} = \left\{ m_{j,r}^{k,i} \right\}_{j,r}$ and $\mathbf{G}_{k,i} = \left\{ g_{j,r}^{k,i} \right\}_{j,r}$, $i = 0, 1$:

(C1) the representation (3) and (4, 5) have to be equivalent, i.e.,

$$\mathbf{G}_{k,r}\, \mathbf{M}_{k,s} = \delta_{r,r}\, \mathbf{I}, \; r, s = 0, 1, \quad \text{and} \quad \mathbf{M}_{k,0}\, \mathbf{G}_{k,0} + \mathbf{M}_{k,1}\, \mathbf{G}_{k,1} = \mathbf{I};$$

(C2) the matrices $\mathbf{M}_{k,i}$, $\mathbf{G}_{k,i}$, $i = 0, 1$ have to be uniformly sparse;

(C3) the matrices $\mathbf{M}_k = (\mathbf{M}_{k,0}, \mathbf{M}_{k,1})$, $\mathbf{G}_k^T = \left( \mathbf{G}_{k,0}^T, \mathbf{G}_{k,1}^T \right)$ have to be spectrally bounded uniformly in $k$;

(C4) the identity $\mathbf{G}_{k,1}\, \mathbf{1} = \mathbf{0}$ holds.

The conditions (C1), (C2) and (C3) guarantee an efficient and stable transformation of the single–scale representation $\mathbf{u}_L = \{u_{L,j}\}_{j \in I_L}$ into the multiscale representation composed of the coarse–scale data $\mathbf{u}_0 = \{u_{0,j}\}_{j \in I_0}$ and a sequence of difference data $\mathbf{d}_k = \{d_{k,j}\}_{j \in J_k}$, $k = 0, \ldots, L-1$, obtained by successive application of (4,5). This transformation can be conversed by (3). The most important feature is condition (C4), which means that the difference coefficients $d_{k,j}$ become small or even vanish in regions where the data vary moderately. Due to this property data compression can be performed. We will see later on how to incorporate this into an adaptive strategy. For the construction of appropriate coefficients, we refer to those known from literature (see e.g. [5, 4, 2, 3]). We want to emphasize that, by the definition of the average (2) and the nestedness of the grids, the coefficients $g_{j,r}^{k,0}$ are uniquely determined by the grid hierarchy.

## 3. Multiscale Transformation and Adaptivity

The single–scale representation $\mathbf{u}_L$ can be transformed into a multiscale representation $\mathbf{u}_{L,MR} = (\mathbf{u}_0, \mathbf{d}_0, \ldots, \mathbf{d}_{L-1})$ applying (4,5) and this operation is conversed using (3). The complexity of this transformation, i.e., the number of operations, is proportional to the number of cells $\# I_L$ of the finest grid, which is optimal, if you are interested in an *exact* transformation. From a numerical point of view, this is no longer desirable, since the finest resolution is only needed where strong variations locally occur in the data and elsewhere the changes are moderate. Hence, we are not in general interested in all data of the finest level, but in single–scale coefficients $u_{k,j}$ corresponding to different levels of resolution. In terms of the multiscale coefficients $d_{k,j}$ this means that some of them vanish or become negligibly small. In the following, we will explain how to reduce the complexity of the transformation to the number of non–vanishing multiscale coefficients. To this end, we introduce the sequence of *truncated* multiscale coefficients $\tilde{\mathbf{u}}_{L,MR} = (\mathbf{u}_0, \tilde{\mathbf{d}}_0, \ldots, \tilde{\mathbf{d}}_{L-1})$ where the vectors $\tilde{\mathbf{d}}_k = \{\tilde{d}_{k,j}\}_{j\in\tilde{J}_k}$ are composed of the significant coefficients, i.e., $\tilde{d}_{k,j} = d_{k,j},\ j \in \tilde{J}_k \subset J_k$, iff $|d_{k,j}| > \varepsilon_k$, where the $\varepsilon_k$ are fixed, level–depending tolerances. The number of significant coefficients is given by $\#\, I_0 + \sum_{k=0}^{L-1} \#\, \tilde{J}_k$ which can be much smaller than the number of all coefficients $\#\, I_0 + \sum_{k=0}^{L-1} \#\, J_k$. Corresponding to this truncated multiscale decomposition $\tilde{\mathbf{u}}_{L,MR}$ we define an *adaptive* single–scale representation $\tilde{\mathbf{u}}_{L,SR} = (\tilde{\mathbf{u}}_0, \ldots, \tilde{\mathbf{u}}_L)$ with $\tilde{\mathbf{u}}_k = \{\tilde{u}_{k,j}\}_{j\in\tilde{I}_k}$ composed of the significant coefficients $\tilde{u}_{k,j} = u_{k,j},\ j \in \tilde{I}_k \subset I_k$. Obviously, the number of adaptive single–scale coefficients $\sum_{k=0}^{L} \#\, \tilde{I}_k$ can be much larger than $\#\, I_L$ in the worst case if $\tilde{I}_k = I_k$. Therefore, no one–to–one transformation between $\tilde{\mathbf{u}}_{L,SR}$ and $\tilde{\mathbf{u}}_{L,MR}$ necessarily exists as there is between $\mathbf{u}_{L,MR}$ and $\mathbf{u}_L$. For this purpose, we have to characterize the representation $\tilde{\mathbf{u}}_{L,SR}$. This is based on the fact that we are dealing with averages. Therefore, we demand that the representation is

(A1) *adaptive*, i.e.,

$$\Omega = \bigcup_{k=0}^{L} \bigcup_{j\in\tilde{I}_k} V_{k,j} \text{ with } \mathrm{meas}\,(V_{k,j} \cap V_{k',j'}) = 0,\ (k,j) \neq (k',j') \text{ and}$$

(A2) *compressed*, i.e., $\left(\forall\, r \in J_{k-1}\ :\ m_{j,r}^{k-1,1} \neq 0 \Rightarrow r \notin \tilde{J}_{k-1}\right) \Rightarrow j \notin \tilde{I}_k$.

The basic idea is to define an *associated* grid from the cells $V_{k,j}$ corresponding to the averages $\tilde{u}_{j,k},\ j \in \tilde{I}_k,\ k = 0, \ldots, L$. By condition (A1), this grid is a decomposition of the computational domain $\Omega$. Since the cells belong to different levels, this grid is adaptive. Which cells are chosen for the associated grid, mainly depends on condition (A2). By this condition, the adaptive single–scale and multiscale representations are connected, since $r \notin \tilde{J}_{k-1}$ is equivalent to $|d_{k-1,r}| < \varepsilon_{k-1}$. Demanding condition (A2) without (A1), may result in an associated grid with overlapping cells and (or) gaps. These effects are excluded by (A1). Furthermore, we conclude that $u_{k,j},\ j \in \tilde{I}_k$, can be reconstructed by the coarse–grid data, i.e., $u_{k,j} = \sum_{r\in I_{k-1}} m_{j,r}^{k-1,0} u_{k-1,r}$, where the error is proportional to $\varepsilon_{k-1}$.

In our application to finite volume schemes, we have to switch between adaptive single–scale and multiscale representation. The transformations are summarized in the following. The encoding, i.e., $\tilde{\mathbf{u}}_{L,SR} \to \tilde{\mathbf{u}}_{L,MR}$, consists of three steps for each level $k$ where we initialize $\hat{I}_L := \tilde{I}_L$ and proceed in descending order:

(E1) $U_k^0 := \bigcup_{j\in\hat{I}_{k+1}} \left\{ r \in I_k\ :\ g_{r,j}^{k,0} \neq 0 \right\}$, $U_k^1 := \bigcup_{j\in\hat{I}_{k+1}} \left\{ r \in J_k\ :\ g_{r,j}^{k,1} \neq 0 \right\}$, (E2) $u_{k,j} = \sum_{r\in E^0_{k,j}} g^{k,0}_{j,r}\, u_{k+1,r}, \quad j \in U^0_k \backslash \tilde I_k,$

$d_{k,j} = \sum_{r\in E^1_{k,j}} g^{k,1}_{j,r}\, u_{k+1,r}, \quad j \in U^1_k,$

(E3) $\tilde J_k := \{ j \in U^1_k \;:\; |d_{k,j}| > \varepsilon_k \}, \; \hat I_k := \tilde I_k \cup U^0_k.$

In step (E1), we collect all indices corresponding to single–scale and difference coefficients, respectively, on level $k$, which depend on a significant single–scale coefficient on level $k+1$. Next, we decompose the coefficient $u_{k+1,j}$ according to (4,5), where the summation is only performed for the non–vanishing mask coefficients $\{g^{k,i}_{j,r}\}_{r\in I_{k+1}}$ collected in the sets $E^i_{k,j},\; i = 0,1$. If we access to $u_{k+1,j},\; j \notin \tilde I_{k+1}$, then $u_{k+1,j}$ has to be calculated by recursively applying $u_{k+1,j} = \sum_{r\in I_k} m^{k,0}_{j,r} u_{k,r}$. According to (A2), only coarse–grid coefficients are required on level $k$, whereas the difference coefficients are not significant, i.e., they are smaller than the threshold value $\varepsilon_k$. Due to assumption (A1) and the special structure of $\mathbf{G}_{k,0}$, one has $\Omega = \bigcup_{l=0}^{k-1} \bigcup_{j\in \tilde I_l} V_{l,j} \cup \bigcup_{j\in \hat I_k} V_{k,j}$ after each sweep in $k$ and, thus, $\hat I_0 = I_0$.

The decoding, i.e., $\tilde{\mathbf{u}}_{L,MR} \to \tilde{\mathbf{u}}_{L,SR}$, is more complicated:

(D1) $\tilde I^p_0 := I_0,\; \tilde I^p_{k+1} := \bigcup_{j\in \tilde J_k} \left\{ r \in I_{k+1} \;:\; m^{k,1}_{r,j} \neq 0 \right\},\; k = 0,\dots,L-1$

$u_{k+1,j} = \sum_{r\in D^0_{k,j}} m^{k,0}_{j,r}\; u_{k,r} + \sum_{r\in D^1_{k,j}} m^{k,1}_{j,r}\; d_{k,r},\; j \in \tilde I^p_{k+1},\; k = 0,\dots,L-1$

(D2) 1) $P_L := \emptyset,\; P_k := \bigcup_{j\in \tilde I^p_{k+1}\cup P_{k+1}} \left\{ r \in I_k \;:\; g^{k,0}_{r,j} \neq 0 \right\},\; k = L-1,\dots,0$

2) $R_k := P_k \cap \tilde I^p_k,\; D_{k+1} := \bigcup_{j\in P_k} \left\{ r \in I_{k+1} \;:\; g^{k,0}_{j,r} \neq 0 \right\}$

$S_0 = \emptyset,\; S_{k+1} := D_{k+1} \backslash \left( D_{k+1} \cap \left( \tilde I^p_{k+1} \cup P_{k+1} \right)\right),\; k = 0,\dots,L-1$

3) $u_{k+1,j} = \sum_{r\in D^0_{k,j}} m^{k,0}_{j,r}\, u_{k,r} + \sum_{r\in D^1_{k,j}} m^{k,1}_{j,r}\, d_{k,r},\; j \in S_{k+1},$
$k = 0,\dots,L-1$

4) $\tilde I_L := \tilde I^p_L \cup S_L,\; \tilde I_k := \tilde I^p_k \backslash R_k \cup S_k,\; k = 0,\dots,L-1$

The transformation is performed only locally according to (3) for all single–scale coefficients $u_{k+1,j},\; j \in \tilde I^p_{k+1}$, where a significant contribution of a difference coefficient $d_{k,r}$ has to be taken into account. For efficiency reason, the summation in (D1) is only done for the non–vanishing mask coefficients $\{m^{k,0}_{j,r}\}_{r\in I_k},\; \{m^{k,1}_{j,r}\}_{r\in J_k}$ collected in the sets $D^i_{k,j},\; i = 0,1$. Proceeding this way, the associated grid may contain overlappings or gaps. Hence, assumption (A1) is not satisfied. In a second step, these have to be removed. To this end, we first have to determine all possible overlappings, i.e., for any single–scale coefficient $u_{k+1,j},\; j \in \tilde I^p_{k+1}$, we determine *all* coarse–grid volumes $V_{k',j'}$ with $V_{k+1,j} \subset V_{k',j'}$. This step (D2.1) is successively performed on each level proceeding from fine to coarse. These indices are collected in the sets $P_k$ for all levels $k = 0,\dots L$. Obviously, $P_L$ is empty, since there is no data on a finer level. The sets $R_k,\; k = 0,\dots,L$, contain the indices of $P_k$ that have actually to be removed from $\tilde I^p_k$. If a coarse–grid value $u_{k,j}$ is taken away, the resulting gap associated to the volume $V_{k,j}$ in the computational domain has to be refilled by information on finer levels. These indices are collected in the sets $S_k,\ k=1,\dots,L$, according to (D2.2). Finally, the overlappings are removed from the predictive sets $\tilde{I}_k^p$, (D2.4), and the gaps are refilled by applying the two–scale equation (3), (D2.3). If we access to a not yet calculated coarse grid information $u_{k,j}$ in the summation, we recursively apply the same two–scale equation.

## 4. Adaptive Finite Volume Schemes

We now incorporate the multiscale concept presented in Sec. 3 into a finite volume scheme in one spatial dimension. Proceeding as in [4, 2], the extension to the multidimensional case for structured as well as unstructured grids is straight forward.

In the following, we assume the computational domain $\Omega=[a,b]\subset \mathrm{IR}$ to be uniformly decomposed on each level $k=0,\dots,L$, i.e., $V_{k,j}=[x_{k,j-1},x_{k,j}],\ j=1,\dots,N_k$, determined by the equidistant grid points $x_{k,j}=a+h_k j,\ j=0,\dots,N_k$, with spatial discretization length $h_k=(b-a)/N_k$. The nestedness of the grid hierarchy is guaranteed by demanding $N_{k+1}=2N_k$ or $h_{k+1}=h_k/2$, respectively. Hence, the sets of indices $I_k,\ J_k$ introduced in Sec. 2 are given by $I_k=J_k=\{1,\dots,N_k\}$. Furthermore, the time interval $[0,T]$ is also uniformly discretized by $0=t_0<\dots<t_{\overline{N}}=T,\ \overline{N}\in \mathrm{IN}$, with $\tau=t_n-t_{n-1}=const.$ The ratio of the spatial and temporal discretization length is defined by $\lambda_k:=\tau/h_k$.

The starting point is a finite volume scheme on the finest grid

$$v_{L,j}^{n+1}=v_{L,j}^n-\lambda_L\left[F_{L,j}^n-F_{L,j-1}^n\right],\qquad j\in I_L, \tag{6}$$

by which the average $u_{L,j}^n:=h_L^{-1}\int_{V_{L,j}}u(t_n,x)\,dx$ of the solution $u$ of (1) is approximated by $v_{L,j}^n$. Here, we assume that the numerical flux can be written as

$$F_{L,j}^n:=F(v_{L,i}^n,\ i\in S_{L,j}), \tag{7}$$

where $S_{L,j}\subset I_L$ is the stencil on which the numerical flux $F_{L,j}^n$ is calculated. Except for periodic boundary conditions, one–sided stencils have to be applied near the boundary according to Dirichlet or von Neumann boundary conditions.

First, we apply the multiscale transformation (4,5) to the quantities $v_{L,j}^n$ where we recursively introduce the single–scale coefficients $v_{k,j}^n,\ j\in I_k$, and the difference coefficients $d_{k,j}^n,\ j\in J_k$, of the levels $k=0,\dots,L-1$. Together with (6), we obtain the multiscale coefficients of the new time level

$$v_{0,j}^{n+1} = v_{0,j}^n-\lambda_0\,\delta_{0,j}^n,\ j\in I_0 \tag{8}$$

$$d_{k,j}^{n+1} = d_{k,j}^n-\lambda_{k+1}\,d_{k,j}^n(\delta),\ j\in J_k,\ k=0,\dots,L-1, \tag{9}$$

with the flux balances $\delta_{k,j}^n,\ j\in I_k$, and the corresponding multiscale coefficients $d_{k,j}^n(\delta),\ j\in J_k$, recursively defined by

$$\delta_{k,j}^n:=\frac{\lambda_{k+1}}{\lambda_k}\sum\nolimits_{r\in I_{k+1}}g_{j,r}^{k,0}\,\delta_{k+1,r}^n,\quad d_{k,j}^n(\delta):=\sum\nolimits_{r\in I_{k+1}}g_{j,r}^{k,1}\,\delta_{k+1,r}^n, \tag{10}$$

initialized on level $L$ according to (7) and $\delta^n_{L,j} := F^n_{L,j} - F^n_{L,j-1}$. Since we consider a one–dimensional dyadic grid hierarchy, the flux balances of the coarser levels can be rewritten in terms of the finest level, i.e.,

$$\delta^n_{k,j} = F^n_{k,j} - F^n_{k,j-1} \quad \text{with} \quad F^n_{k,j} := F^n_{L,2^{L-k}j}. \tag{11}$$

Up to now, the system of evolution equations (6) for the averages $v^n_{L,j}$, $j \in I_L$, of the finest level has been *equivalently* transformed into a system of evolution equations (8, 9) for the multiscale coefficients $v^n_{0,j}$, $j \in I_0$, and $d^n_{k,j}$, $j \in J_k$, $k = 0, \ldots, L-1$. The efficiency of the scheme can now be improved by applying a threshold process to the difference coefficients $d^{n+1}_{k,j}$, i.e., the evolution equation (9) is only performed for $j \in \tilde{J}^{n+1}_k \subset J_k$, $k = 0, \ldots, L-1$. Following Harten's original concept [5], the truncation of the difference coefficients, i.e., $d^n_{k,j} := 0$, $j \in J_k \backslash \tilde{J}^{n+1}_k$, can be used to *replace* the calculation of certain coarse–grid fluxes $F^n_{k,j}$ according to (10) by a linear combination of already calculated numerical fluxes of the coarser level $k-1$ (see [5, 2, 3]). This leads to a *hybrid* scheme where only a few terms are computed according to (7) and (11) and the remaining fluxes are calculated by difference formulae. In general, this accelerates the computation, if the calculation of (7) is sufficiently expensive. For more details see [5, 4, 2]. However, the complexity of the scheme still remains that of the *finest* level (see e.g. [2]). This is essentially based on the fact that the numerical fluxes $F^n_{k,j}$ which have to be computed by (11) are calculated from the data $v^n_{L,j}$ of the finest level. In order to reduce the complexity of the computation, we have to proceed differently. The main idea is to compute the numerical fluxes not necessarily from the single–scale coefficients $\mathbf{v}^n_L$ of the finest level but from the adaptive single–scale representation $\tilde{\mathbf{v}}^n_{L,SR}$ defined according to $\tilde{\mathbf{u}}_{L,SR}$ introduced in Sec. 3. This results in an *adaptive* instead of an hybrid scheme:

(S1) Decoding: $\tilde{\mathbf{v}}^n_{L,MR} \rightarrow \tilde{\mathbf{v}}^n_{L,SR} = (\tilde{\mathbf{v}}^n_0, \ldots, \tilde{\mathbf{v}}^n_L)$ with $\tilde{\mathbf{v}}^n_k = \{v^n_{k,j}\}_{j \in \tilde{I}^n_k}$

(S2) Prediction of $\tilde{J}^{n+1}_k$, $k = 0, \ldots, L-1$, according to [5]

(S3) $\overline{v}^n_{L,i} := v^n_{k,j}$ with $j \in \tilde{I}^n_k$, $V_{L,i} \subset V_{k,j}$, $\forall\, i \in \bigcup_{j \in F_n} S_{L,j}$,

$F_n := \left\{ j\, 2^L \ : \ j \in I_0 \right\} \cup \bigcup_{k=0}^{L-1} \bigcup_{j \in \tilde{J}_k} \left\{ (r-1)\, 2^{L-k-1} \ : \ r \in E^1_{k,j} \right\}$

(S4) $F^n_{L,j} = F(\overline{v}^n_{L,i}\ ;\ i \in S_{L,j})$, $\quad j \in F_n$

(S5) $v^{n+1}_{0,j} = v^n_{0,j} - \lambda_0\, \delta^n_{0,j}$, $\quad j \in I_0$

$d^{n+1}_{k,j} = d^n_{k,j} - \lambda_{k+1} \sum_{r \in E^1_{k,j}} g^{k,1}_{j,r}\, \delta^n_{k+1,r}$, $\quad j \in \tilde{J}^{n+1}_k$, $0 \le k \le L-1$

Each time step is composed of five steps where a sequence of truncated multiscale coefficients $\tilde{\mathbf{v}}^n_{L,MR} = (\tilde{\mathbf{v}}^n_0, \tilde{\mathbf{d}}^n_0, \ldots, \tilde{\mathbf{d}}^n_{L-1})$ with $\tilde{\mathbf{d}}^n_k = \{d^n_{k,j}\}_{j \in \tilde{J}^n_k}$ is supposed to be known at time level $t_n$. Herein, $\tilde{\mathbf{v}}^n_{L,MR}$ is defined according to $\tilde{\mathbf{u}}_{L,MR}$ introduced in Sec. 3. In a first step (S1) we decode the sequence of truncated multiscale coefficients into a sequence of adaptive single–scale coefficients according to (D1, D2) such that (A1, A2) hold. Since $\tilde{\mathbf{v}}^{n+1}_{L,MR}$ is not yet known, we next determine a prediction of $\tilde{J}_k^{n+1},\ k = 0, \dots, L-1$, from $\tilde{\mathbf{v}}^n_{L,MR}$. Here, we follow Harten's original concept [5]. This is based on the finite speed of propagation which is characteristic for hyperbolic problems. For more details see [2, 4]. The most important step of our algorithm is the projection of the single–scale coefficients of the coarser levels to the finest level (S3). This projection is unique, since the representation $\tilde{\mathbf{v}}^n_{L,SR}$ is supposed to satisfy (A1). Of course, we do not calculate all coefficients $\overline{v}^n_{L,j}$ of the finest level, but only those which are needed in the calculation of the numerical fluxes according to (11). To this end, we introduce the set $F_n$ which consists of all indices corresponding to the required coefficients. From the projection $\hat{v}_L$, we now calculate the numerical fluxes (S4) according to definition (7). Finally, we can calculate the multiscale coefficients of the the new time level, (S5). Once again, the summation is only performed for those coefficients which give a non–vanishing contribution, i.e., $g^{k,1}_{j,r} \neq 0$.

## 5. Numerical Calculations

In the following, we want to present preliminary results of the adaptive algorithm applied to Burgers' equation neglecting viscosity, i.e., $f(u) = 0.5\,u^2$, and periodic initial data $u_0(x) = \sin(\pi x),\ x \in \Omega := [0, 2]$. Hence, a stationary shock develops at time $t_s = 1/\pi$ in position $x_s = 1$. We always choose $T = 0.4$. The exact solution is plotted in Fig. 1. The underlying finite volume scheme is a second order ENO scheme using polynomial reconstruction of degree 1 and an exact Riemann solver (see [6]). For all computations, we have chosen $N_0 = 20$ intervals on the coarsest level such that there are $N_L = N_0\,2^L$ intervals on the finest level according to the dyadic grid hierarchy. Correspondingly, the time discretization length is chosen such that the CFL number is always equal to 0.8 on the finest level. This corresponds to $\overline{N}_L = 5 \times 2^L$ time steps depending on $L$. Furthermore, the coefficients $m^{k,i}_{j,r}$ and $g^{k,i}_{j,r}$, respectively, are determined by a polynomial reconstruction of degree 2 (see [4]). According to Sec. 3, the truncation of the multiscale decomposition is applied with the threshold values $\varepsilon_{L-1} = 0.01,\ \varepsilon_k = 0.7\,\varepsilon_{k+1},\ k = L-2, \dots, 0$. All computations have been performed on an SGI O2 workstation.

As an example, the approximation is presented for $L = 14$ in Fig. 1. It is in good agreement with the exact solution, although the finest level is only involved close to the shock as can be seen from the level distribution $\tilde{I}_k,\ k = 0, \dots, L$, of the adaptive single–scale coefficients (Fig. 2). In addition, the distribution $\tilde{J}_k,\ k =$

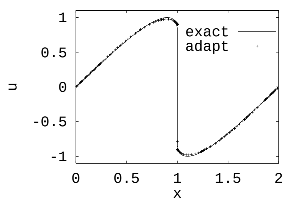


FIGURE 1.

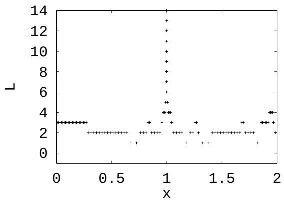


FIGURE 2.

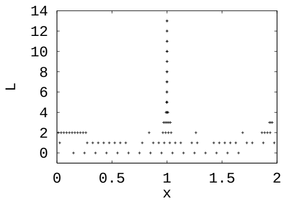


FIGURE 3.

| L | $N_L$ | $D_{max}$ | $F_{max}$ | $C_{MR}$ | $C_{FV}$ | $S_{MR}$ |
|---|---|---|---|---|---|---|
| 10 | 20480 | 186 | 73 | 233.3 | 419.9 | 1.80 |
| 11 | 40960 | 232 | 77 | 704.4 | 1975.0 | 2.80 |
| 12 | 81920 | 261 | 81 | 1746.3 | 8943.3 | 4.77 |
| 13 | 163840 | 295 | 81 | 4362.9 | 38152.5 | 8.74 |
| 14 | 327680 | 362 | 89 | 12388.0 | 153936.8 | 12.43 |

TABLE 1.

$0, \ldots, L-1$, of the corresponding multiscale coefficients is shown in Fig. 3. Here, the indices $j \in \tilde{I}_k$ and $j \in \tilde{J}_k$, respectively, are plotted with respect to the cell centers $\hat{x}_{k,j}$ of the corresponding intervals $V_{k,j}$. We notice that the smooth regions of the solution are, in fact, resolved by coarse levels, whereas the higher levels are only required close to the shock position $x_s$. This implies that the scheme is capable to resolve appropriately effects proceeding on different scales. Similar results are reported by other authors following Harten's concept (see [5, 7, 2]).

Furthermore, we are interested in the complexity of our scheme. To this end, we have performed several calculations refining the finest level, i.e., $L = 10, \ldots, 14$. The results are presented in Tab. 1. As a measure of the complexity, we introduce the maximum number $D_{max}$ and $F_{max}$ of significant multiscale coefficients, i.e., $\# I_0 + \sum_{k=0}^{L-1} \# \tilde{J}_k^n$, and of the calculated numerical fluxes, i.e., $\# F_n$, with respect to all time steps $n = 0, \ldots, \overline{N}_L$. We notice that the numbers $D_{max}$ and $F_{max}$, respectively, increase with $L$. This corresponds to the additional highest–scale coefficients close to the shock and a larger threshold value $\varepsilon_k$ on the coarser levels. Moreover, these numbers are correlated. This is different to Harten's concept [5] where the number $D_{max}$ corresponds to the number of original fluxes, but not to the number of all fluxes including the interpolated fluxes. Hence, following Harten's approach the computation can only be accelerated by a factor about 2–3 (see [2]) depending on the underlying finite volume scheme. Opposite to this, we achieve much higher speed–up factors as recorded in Tab. 1. For this, we have additionally performed the computation with the original finite volume scheme. By this the speed–up factor $S_{MR}$ can be introduced as the ratio of the computational times corresponding to the original and the adaptive scheme, $C_{FV}$ and $C_{MR}$. Here, the computational time is measured in CPU seconds. We notice that the speed–up factor increases with higher levels. This is based on the fact that $C_{FV}$ increases by a factor of almost 4 corresponding to the refining of the spatial and temporal discretization lengthes by a factor of 2. However, $C_{MR}$ only increases by an averaged factor of about 2.5 which is almost optimal, since the number of time steps is doubled. Thus, we conjecture that, theoretically, an arbitrary speed–up factor can be achieved for $L \to \infty$, since the complexity of the algorithm corresponds to that of the significant multiscale coefficients. This is not true for Harten's concept, where it has been proved that $S_{MR}$ tends to a finite number for $L \to \infty$ (see [4, 2]).

## 6. Conclusion

In the present paper, we have introduced a new adaptive concept for finite volume schemes. Here, adaptivity is controlled by local multiscale decompositions. First test calculations have shown that the complexity of the resulting algorithm corresponds to the number of non–vanishing multiscale coefficients. This is an essential improvement of Harten's original idea of an hybrid scheme. Additionally, further investigations have already shown that this concept can also be applied to inhomogeneous conservation laws.

Our future work is devoted to time adaptivity. Presently, the temporal discretization length is significantly restricted by the CFL number because of a very small number of significant multiscale coefficients of the finest level. This constraint becomes even more serious if more levels are involved, i.e., $L \gg 1$. In order to overcome this obstruction, we want to combine our present concept with a local time–stepping strategy.

## 7. Acknowledgement

The authors are supported in parts by the DFG in the Collaborative Research Center SFB 401 at the University of Technology Aachen.

## References

[1] B. Bihari and A. Harten, *Multiresolution schemes for the numerical solution of 2–D conservation laws I,* SIAM J. Sci. Comput., **18 (2)** (1997), 315–354.

[2] B. Gottschlich–Müller, *Multiscale Schemes for Multidimensional Conservation Laws,* PhD thesis, RWTH Aachen, 1998, submitted.

[3] B. Gottschlich–Müller and S. Müller, *Application of multiscale techniques to hyperbolic conservation laws,* Numerical Treatment of Multi–scale Problems, Proceedings of the 13th GAMM–Seminar held in Kiel, January 24–26, 1997, submitted.

[4] B. Gottschlich–Müller and S. Müller, *On multi–scale concepts for multi–dimensional conservation laws,* Proceedings of Guangzhou International Symposium on Computational Mathematics held in Guangzhou, August 11–15, 1997, to appear.

[5] A. Harten, *Multiresolution algorithms for the numerical solution of hyperbolic conservation laws,* Comm. Pure Appl. Math., **48 (12)** (1995), 1305–1342.

[6] A. Harten, B. Engquist, S. Osher and S. R. Chakravarthy, *Uniformly high order accurate essentially non–oscillatory schemes III,* J. Comp. Phys., **71** (1987), 231–303.

[7] B. Sjögreen, *Numerical experiments with the multiresolution scheme for the compressible Euler equations,* J. Comp. Phys., **117** (1995), 251–261.

Institut für Geometrie und Praktische Mathematik,
RWTH Aachen,
D-52056 Aachen, Germany
*E-mail address*: `mueller@igpm.rwth-aachen.de`